Farver, O., & Pecht, I. (1981b) *Proc. Natl. Acad. Sci. U.S.A. 78*, 4190–4193.
French, T. C., & Hammes, G. G. (1965) *J. Am. Chem. Soc. 87*, 4669.
Gudat, J. C., Singh, J., & Wharton, D. C. (1973) *Biochim. Biophys. Acta 292*, 376–381.
Hill, H. A. O., & Smith, B. E. (1979) *J. Inorg. Biochem. 11*, 79–86.
Kuronen, T., & Ellfolk, N. (1972) *Biochim. Biophys. Acta 275*, 308–315.
Mitra, S., & Bersohn, R. (1982) *Proc. Natl. Acad. Sci. U.S.A.* (in press).
Parr, S. P., Barber, D., Greenwood, C., Phillips, B. W., & Melling, J. (1976) *Biochem. J. 157*, 423–430.
Pecht, I., & Rosen, P. (1973) *Biochem. Biophys. Res. Commun. 50*, 853–858.
Powell, M. J. D. (1971) in Harwell Subroutine Library, subroutine VA04A, A.E.R.E., Harwell, U.K.
Rigler, R., Rabl, C. R., & Jovin, T. M. (1974) *Rev. Sci. Instrum. 45*, 580–585.
Rosen, P. (1977) Ph.D. Thesis, The Feinburg Graduate School of the Weizmann Institute of Science, Rehovot, Israel.
Rosen, P., & Pecht, I. (1976) *Biochemistry 15*, 775–786.
Rosen, P., Segal, M., & Pecht, I. (1981) *Eur. J. Biochem. 120*, 330–344.
Silvestrini, M. C., Brunori, M., Wilson, M. T., & Darley-Usmar, V. M. (1981) *J. Inorg. Biochem. 14*, 327–338.
Ugurbil, K., & Bersohn, R. (1977) *Biochemistry 16*, 3016–3019.
Wherland, S., & Pecht, I. (1978) *Biochemistry 17*, 2585–2591.
Wilson, M. T., Greenwood, C., Brunori, M., & Antonini, E. (1975) *Biochem. J. 145*, 449–457.
Yamanaka, T., & Okunuki, K. (1963) *Biochim. Biophys. Acta 67*, 379–385.
Zidovetzki, R., Blatt, Y., Glaudemans, C. P. J., Manjula, B. N., & Pecht, I. (1980) *Biochemistry 19*, 2790–2795.

Properties of the Prosthetic Groups of Rabbit Liver Aldehyde Oxidase: A Comparison of Molybdenum Hydroxylase Enzymes†

Michael J. Barber, Michael P. Coughlan,‡ K. V. Rajagopalan, and Lewis M. Siegel*

ABSTRACT: Rabbit liver aldehyde oxidase (AO), like milk xanthine oxidase (XO) and chicken liver xanthine dehydrogenase (XDH), possesses the following prosthetic groups: FAD, a functional Mo center, and two spectroscopically distinct iron–sulfur centers, one with $g_{av} < 2.0$ (termed Fe/S I) and the other with $g_{av} > 2.0$ (termed Fe/S II) in the reduced enzyme. EPR spectra for the Mo^V species were found to be nearly identical in AO and XO for a number of enzyme complexes, and the midpoint reduction potentials for functional Mo^{VI}/Mo^V (−359 mV) and Mo^V/Mo^{IV} (−351 mV) were nearly the same in all three enzymes (50 mM phosphate, pH 7.8). A strong magnetic interaction between Mo^V and reduced Fe/S I, previously detected in XO and XDH, was also found in AO. No Mo^V–Fe/S II interaction could be detected in AO (nor in XO). In contrast, the order of reduction of Fe/S I and Fe/S II, as measured from their midpoint potentials, is reversed in AO (E_m = −207 and −310 mV, respectively) as compared to XO (E_m = −280 and −245 mV, respectively) in phosphate buffer at pH 7.8. The oxidized–reduced extinction coefficients at 450 and 550 nm for the two centers are also apparently reversed in AO and XO. Although magnetic interaction between FAD and one or both reduced Fe/S centers has been detected in both AO and XO, no magnetic interaction between the two reduced Fe/S centers themselves was found in AO (although such interaction has been seen in XO). The average FAD reduction potential is substantially more positive in AO (E_m for FAD/FADH·, −258 mV; FADH·/$FADH_2$, −212 mV at pH 7.8) than in XO or XDH. It can be concluded that although the properties and immediate environment of the functional Mo center are conserved in the three Mo hydroxylase enzymes, and all three enzymes possess the same set of prosthetic groups, the properties of the groups which transfer electrons from the Mo to the ultimate electron acceptor can vary substantially in AO, XO, and XDH.

Milk xanthine oxidase (XO)[1] and avian liver xanthine dehydrogenase (XDH) each contain two subunits (M_r 140000) (Coughlan, 1980). Each subunit contains one FAD, one Mo center with a novel pterin cofactor (Johnson et al., 1980), and two spectroscopically distinct Fe_2S_2 centers, termed Fe/S I and Fe/S II, which differ in their EPR properties (Bray, 1975), reduction potentials (Cammack et al., 1976; Barber et al., 1980), and visible absorption spectra (Olson et al., 1974b).

Rabbit liver aldehyde oxidase, which differs markedly in its substrate specificity from XO and XDH (Feldsted et al., 1973; Coughlan, 1980), apparently contains a similar molecular structure [M_r 280000; two FAD, two Mo, and eight non-heme Fe (Rajagopalan et al., 1962)]. The Mo center of AO contains a pterin cofactor like that found in XO/XDH (Johnson, 1980). In its functional form, the AO Mo center contains a cyanolyzable sulfur atom (Branzoli & Massey, 1974a) which EXAFS (Bordas et al., 1980; Cramer et al., 1981) and EPR studies (Malthouse & Bray, 1980) have shown to be due to

† From the Department of Biochemistry, Duke University School of Medicine, and the Veterans Administration Hospital, Durham, North Carolina 27705. *Received January 28, 1982.* This work was supported by Grants AM-13460 (to L.M.S.) and GM-00091 (to K.V.R.) from the National Institutes of Health and Project Grant 7875-01 (to L.M.S.) from the Veterans Administration.

‡ Permanent address: Department of Biochemistry, University College, Galway, Ireland.

[1] Abbreviations: AO, rabbit liver aldehyde oxidase; Fe/S I, iron–sulfur center with $g_{av} < 2.0$ in the reduced enzyme; Fe/S II, iron–sulfur center with $g_{av} > 2.0$ in the reduced enzyme; XO, milk xanthine oxidase; XDH, avian liver xanthine dehydrogenase; EXAFS, X-ray absorption fine structure, extended; EDTA, ethylenediaminetetraacetic acid.

0006-2960/82/0421-3561$01.25/0

a Mo=S structure in XO and XDH.

Rajagopalan et al. (1968a,b) showed that AO exhibited EPR signals, upon reduction with substrates or dithionite, which were associated with Mo^V, FAD semiquinone, and a reduced Fe/S center. Rapid kinetic studies indicate that reduction of these centers could occur at rates consistent with their participation in catalysis. Branzoli & Massey (1974a,b) provided evidence that the oxidation of aldehydes and *N*-methylnicotinamide occurrred at the Mo center, while reduction of oxygen occurred at the FAD, a reaction sequence analogous to that proposed for reaction of XO with substrates (Olson et al., 1974a,b).

In recent years, a great deal of work has been devoted to elucidation of the detailed structure and reaction mechanisms of the xanthine oxidizing Mo hydroxylases (Bray, 1980a). In particular, the nature of the Mo ligands in active and inactive enzyme forms and in complexes with substrates (Bray, 1980b), the role of H transfer involving the Mo center in oxidation–reduction reactions (Gutteridge et al., 1978; Barber & Siegel, 1982), the relative spatial arrangements of the various electron-carrying groups within the enzyme subunit (Lowe & Bray, 1978; Barber et al., 1982), the reduction potentials of the various prosthetic groups (Cammack et al., 1976; Barber et al., 1980; Barber & Siegel, 1982), and a detailed mechanism for electron flow within the enzyme based solely on the relative potentials of the prosthetic groups (Olson et al., 1974b) have all been elucidated to varying degrees of certainty with XO and/or XDH.

The study of AO, in contrast, has been relatively neglected. With the belief that understanding of the mechanism of Mo hydroxylase function could be furthered by a systematic comparison of AO with XO and XDH, we have undertaken an investigation of some spectroscopic and potentiometric properties of the various prosthetic groups in AO. The present work reports that AO, like XO and XDH, contains two distinct Fe/S centers but that the reduction potentials and optical properties of the centers, as well as the degree of magnetic interaction between them, differ markedly in AO vs. XO/XDH. The FAD is much more easily reduced in AO than in XO or XDH, and the magnitude of the FAD–Fe/S center magnetic interaction is much weaker in AO. The Mo center, in contrast, is similar in all three enzymes (despite the differences in substrate specificity), and the strong Mo–Fe/S I magnetic interaction seen in XO and XDH (Lowe & Bray, 1978) is also present in AO.

Experimental Procedures

Standard Buffer. Potassium phosphate (0.05 M), pH 7.8, containing 1 mM EDTA, was used in all experiments.

Enzyme. Aldehyde oxidase was purified from fresh rabbit livers according to the procedure of Rajagopalan et al. (1962). Enzyme concentration was determined from the absorbance at 450 nm, using E_{450} = 69 mM^{-1} cm^{-1}. Enzyme concentrations used in the experiments described in this work were in the range 20–100 μM. Total active center concentrations (functional plus nonfunctional) were taken to be twice the enzyme concentration. The concentrations of all enzyme species except "rapid" Mo^V were related to the concentration of total enzyme active centers. The proportion of enzyme centers which contained functional Mo was determined on the basis of the activity/A_{450} ratio as described by Branzoli & Massey (1974a). Using the ratio determined by them for fully functional enzyme, we found that the AO preparation used in this work contained 30% functional Mo centers. In potentiometric titrations, the fraction of rapid Mo^V observed is calculated by dividing the concentration of rapid Mo^V by the concentration of functional Mo centers.

Desulfo AO was prepared as described by Branzoli & Massey (1974a). The formaldehyde, methanol, and desulfo ethylene glycol adducts of AO were prepared by procedures previously described for the formation of the analogous adducts in XO (Pick et al., 1971; Lowe et al., 1976).

Xanthine oxidase and its desulfo derivative were prepared, and the concentrations of its various centers were determined as described by Barber & Siegel (1982).

Spectra. Optical spectra were recorded in quartz cells or EPR tubes with an Aminco DW-2 spectrophotometer equipped with a microcondenser.

EPR spectra were recorded at X band on a Varian E9 spectrometer equipped with variable temperature accessory and using modulation at 100 kHz. Measurements at temperatures <80 K were made by using a liquid He cryostat (Air Products). For quantitation of reduced Fe/S I centers, spectra were recorded at 40 K, 1-mW power, and 1-mT modulation amplitude, and the height of the g_2 feature above the base line was measured. For quantitation of reduced Fe/S II centers, spectra were recorded at 20 K, 100-mW power, and 1-mT modulation amplitude, and the height of the g_1 feature was measured. FAD radical and Mo^V center signals were normally recorded at 173 K and 0.25-mT modulation amplitude under nonsaturating conditions of power. Double integration of signals was performed with Cu-EDTA as standard. Signals were normalized as described by Barber & Siegel (1982).

"Resting II" Mo^V was measured by means of the amplitude of its g_2 feature below the base line. Rapid Mo^V was determined from the height of the g_1 feature at a position where the presence of resting II Mo^V did not contribute to the spectrum, using samples that contained negligible "slow" Mo^V signals. Slow Mo^V was measured by means of the intensity of its g_3 feature, one which shows no contribution from either resting II or rapid Mo^V. Quantitation of rapid Mo^V spectra was performed both by subtraction of the integrated resting II and slow Mo^V spectra from the overall Mo^V spin concentration and by comparison of the measured signal intensity with standard spectra of XO containing mixtures of comparable Mo^V species. Both methods gave nearly identical results.

Simulations and substractions of experimental EPR spectra were performed with the aid of a Hewlett-Packard 9825A computer, 9874A digitizer, and 7225A plotter. The simulation program used was a modified version of that described by Lowe (1978).

Experimental data for EPR signal intensity (S) obtained as a function of incident microwave power (P) were fitted to the semiempirical equation of Beinert & Orme-Johnson (1967): $\log S/\sqrt{P} = \log k - 0.5b \log [1 + P/P_{1/2}]$, where $P_{1/2}$, k, and b are constants. For any one species examined, the value of b (the "inhomogeneity" parameter) was set to a constant value and $P_{1/2}$ varied as the concentration of a second paramagnetic center was changed. For details see Barber et al. (1982).

Potentiometric Titrations. Potentiometric titrations were carried out at 25 °C in an anaerobic cell of the type described by Dutton (1971). Enzyme samples were equilibrated with the gold indicating electrode with the aid of a mixture of dye mediators, the solution being poised at a series of desired potentials by addition of small volumes of 0.1 M $Na_2S_2O_4$ or 0.2 M $K_3Fe(CN)_6$ solutions. After equilibration at each potential (5 min for most samples, 30 min for the desulfo Mo center), an aliquot of enzyme was removed into a gas-tight Hamilton syringe, transferred to an Ar-flushed EPR tube, and frozen in liquid N_2 for subsequent EPR analysis. Details of

Table I: Parameters of Various EPR-Detectable Species in Aldehyde Oxidase and Milk Xanthine Oxidase[a]

species	aldehyde oxidase g values (A values, mT)	xanthine oxidase g values (A values, mT)
FADH·	2.0036	2.0035[b]
reduced Fe/S I	2.018, 1.930, 1.918	2.022, 1.935, 1.899[c]
reduced Fe/S II	2.106, 2.003, 1.915	2.12, 2.007, 1.91[d]
Mo^V		
resting II	1.9790, 1.9720, 1.9630	
glycol-inhibited desulfo	1.9803, 1.9713, 1.9634	1.9784, 1.9707, 1.9644[e]
methanol-inhibited	1.9942 (0.61), 1.9787 (0.60), 1.9517[f] (0.63)	1.9911 (0.50), 1.9772 (0.34), 1.9513[g] (0.54)
desulfo (slow)	1.9713 (1.55), 1.9671 (1.43), 1.9554 (1.48)	1.9719 (1.66, 0.16), 1.9671 (1.66, 0.16), 1.9551[h] (1.56, 0.16)

[a] g (±0.0005) and A (±0.01 mT) values were obtained by comparison of experimental and computer simulated spectra. For details of formation of the various species, see Figure 7 and the text. [b] Bray & Vanngard (1969). [c] Gibson & Bray (1972). [d] Lowe et al. (1972). [e] Bray (1980b). [f] Formaldehyde-inhibited aldehyde oxidase yielded identical Mo^V EPR parameters. [g] Tanner et al. (1978). [h] Gutteridge et al. (1978). Values for both a strongly and weakly coupled proton were detected.

the titration procedure are described by Cammack et al. (1976) and Barber & Siegel (1982).

Reduction midpoint potentials, expressed relative to the standard hydrogen electrode, were obtained by fitting the experimental titration data with theoretical Nernst curves for either a single $n = 1$ reduction process (the Fe/S centers) or the intermediate species formed in two consecutive $n = 1$ reduction processes (the FADH· and Mo^V centers) using a statistical least-squares fitting program. For details see Barber et al. (1980). As discussed by these authors, the magnitude of the errors associated with the measured midpoint potentials can be expected to be ±15 mV.

Freeze Quenching. Freeze-quenched samples were prepared for EPR analysis by using an Update Instruments System 1000 precision ram system using procedures described by Barber & Salerno (1980).

Results

Fe/S Centers. (A) EPR Spectra. Fe/S I and II in XO were characterized originally by means of their EPR spectral characteristics [see Bray (1975) for review]. Fe/S I is of near axial symmetry, with $g_{av} = 1.95$; as seen in Table I, only one of its g values is above the value for the free electron. Its EPR spectrum is readily observable at 70–100 K, and if examined at 20 K is relatively easily saturated with microwave power. In contrast, Fe/S II in XO has rhombic symmetry, with $g_{av} = 2.01$. It is unique among known Fe_2S_2 centers in having two of its g values in the reduced state at or above the value for the free electron (Table I). It is virtually undetectable at $T > 60$ K and is difficult to saturate with microwave power at 20 K.

Figure 1A shows an EPR spectrum of fully reduced AO taken at 20 K and low microwave power (1 mW). The spectrum is dominated by that of an Fe/S center (although features due to highly saturated Mo^V and FADH· are seen in the central portion of the spectrum), nearly axial in shape, with $g_{av} = 1.96$. A computer simulation of this spectrum (assuming an isotropic line width of 1.6 mT), shown in Figure 1B, yielded best fit g values of 2.018, 1.930, and 1.918 (Table I). Integration of this spectrum showed this center to account for one electron spin per FAD. The temperature dependence of this Fe/S center spectrum, defined by the height of the $g = 1.930$ feature above the base line (a position at which Fe/S II does not interfere) and recorded at low (0.1 mW) microwave power, shows that, although maximum intensity is reached at 25–45 K, the spectrum is still easily observed at 70 K (Figure 2), albeit in a somewhat broadened form. Figure 3A shows that this center was saturated at $P_{1/2} = 17$ mW at 20 K. XO center Fe/S I exhibited a $P_{1/2} = 20$ mW (with Fe/S II oxidized) under the same conditions. Thus, the $g_{av} = 1.96$ Fe/S center of AO can be equated, on the basis of its EPR prop-

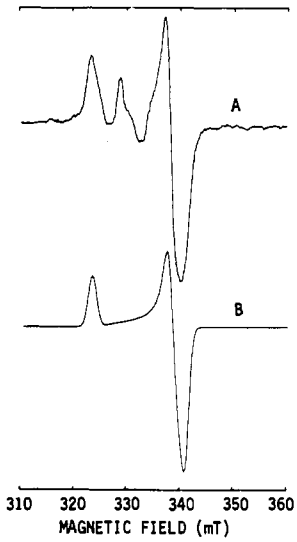

FIGURE 1: EPR spectrum of reduced Fe/S I in aldehyde oxidase. (A) A solution of 18 μM AO in standard buffer was poised at −500 mV with $Na_2S_2O_4$ as reductant. Conditions of spectroscopy: temperature, 20 K; microwave frequency, 9.16 GHz; microwave power, 1 mW; modulation amplitude, 1 mT. (B) Computer simulation of reduced Fe/S I center spectrum using $g = 2.018$, 1.930, and 1.918 and an isotropic line width of 1.6 mT.

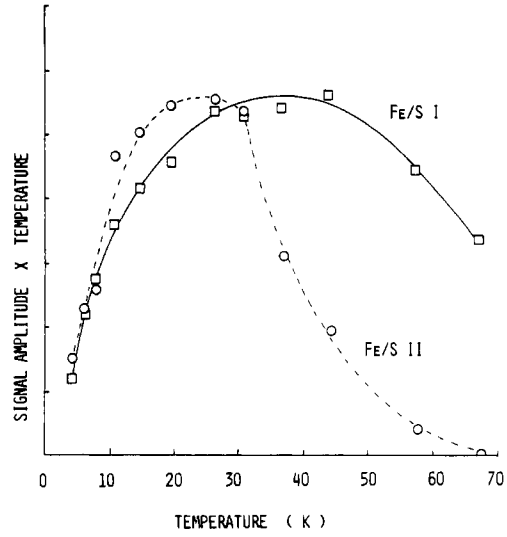

FIGURE 2: Temperature dependence of reduced iron–sulfur center EPR spectra in aldehyde oxidase. A solution of 100 μM AO in standard buffer was reduced with 5 mM $Na_2S_2O_4$, and EPR spectra were recorded at a series of temperatures. For Fe/S I (□), spectra were recorded at 0.1 mW power, and the height of the $g = 1.930$ feature above the base line was measured. For Fe/S II (○), spectra were recorded at 1 mW power, and the height of the $g = 2.106$ feature was measured.

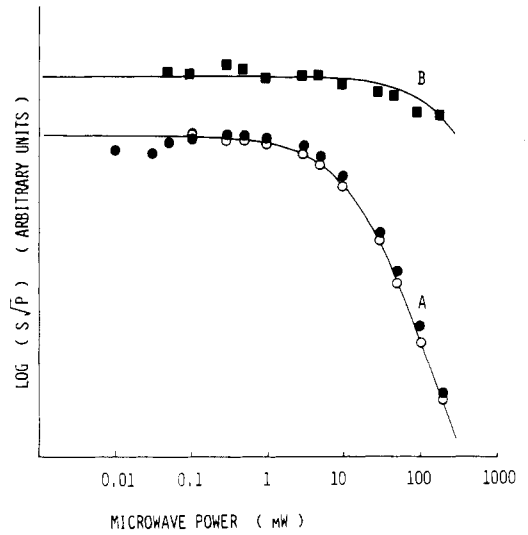

FIGURE 3: Microwave power saturation behavior of reduced iron–sulfur center spectra in aldehyde oxidase. Spectra were recorded under the conditions of Figure 1, except that the microwave power was varied. (A) Reduced Fe/S I. The intensity of the $g = 1.930$ feature above the base line was measured. (●) AO poised at −400 mV. (○) AO poised at −186 mV. (B) Reduced Fe/S II (■). The intensity of the $g = 2.106$ feature was measured in AO poised at −400 mV.

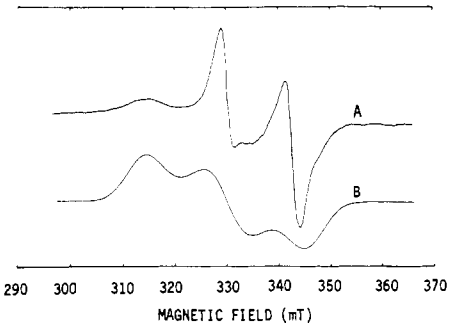

FIGURE 4: EPR spectrum of reduced Fe/S II in aldehyde oxidase. (A) Enzyme was prepared and the spectrum recorded as in Figure 1, except that the microwave power was 400 mW. The spectrum retains features of reduced Fe/S I (see Figure 1) which could largely be eliminated by subtracting a suitably weighted spectrum like that of Figure 1B from that shown. (B) Computer simulation of reduced Fe/S II center spectrum using $g = 2.106$, 2.003, and 1.915 and an isotropic line width of 6 mT.

erties, with the Fe/S I center of XO. We shall refer to this center then as Fe/S I.

Figure 4A shows an EPR spectrum of fully reduced AO taken at 20 K and high microwave power (400 mW). At this power, the features due to Fe/S I, although still present, are highly saturated, and one can detect the presence of a second, considerably broader, Fe/S center, rhombic in shape, with $g_{av} = 2.01$. The line shape of this Fe/S center component of Figure 4A, most easily seen by means of the prominent broad g_1 feature at 315 mT and the shoulder due to broad g_3 feature at 345 mT, was determined by incremental subtraction of a spectrum of Fe/S I (Figure 1A) from that of Figure 4A until the sharp g_2 feature at 342 mT due to this center was abolished. A computer simulation of the resulting Fe/S center spectrum, shown in Figure 4B, gave best-fit g values of 2.106, 2.003, and 1.915 (Table I). Integration of this spectrum showed it to account for one electron spin per FAD. Figure 2 shows that the intensity of the Fe/S II center spectrum (measured by means of the $g = 2.106$ feature), recorded at low microwave power (1 mW), reached maximum intensity at 20–30 K and was not observable at 70 K. Figure 3B shows that this center was saturated at $P_{1/2} = 300$ mW at 20 K. XO

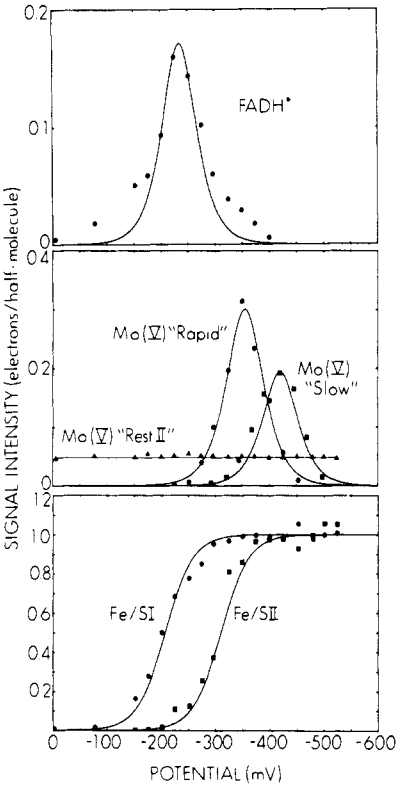

FIGURE 5: Behavior of the FAD semiquinone, Mo^V rapid, slow, and resting II, and reduced Fe/S I and Fe/S II center EPR signals on potentiometric titration of AO at pH 7.8. For all curves, signal intensity is plotted as a function of potential with respect to the standard hydrogen electrode. The experiments were performed as indicated under Experimental Procedures. All signals were measured with solutions containing 18 μM AO, except for the Mo^V slow species, which was determined with 7 μM desulfo AO. Theoretical curves for FADH· and Mo^V species represent the amount of intermediate species present in two consecutive $n = 1$ reduction processes with midpoint potentials given in Table II. Theoretical curves for reduced Fe/S centers represent the amount of reduced species formed in single $n = 1$ reduction processes with midpoint potentials given in Table II.

center Fe/S II gave $P_{1/2} = 500$ mW in a parallel study. Thus the $g_{av} = 2.01$ Fe/S center of AO can be equated, on the basis of its EPR properties, with the Fe/S II center of XO. We shall refer to this center then as Fe/S II.

Figure 3 also shows the saturation behavior of Fe/S I at 20 K in a sample of AO poised at a potential (−186 mV) at which Fe/S I is partially reduced, but no reduction of Fe/S II could be detected (see below). It can be seen that there is no effect of Fe/S II center reduction on the saturation properties of Fe/S I in AO. This result is in marked contrast to the 2.5-fold increase in $P_{1/2}$ of Fe/S I seen in XO when Fe/S II in that enzyme is reduced (Barber et al., 1982). Thus, the degree of magnetic interaction between the Fe/S centers differs significantly in the two enzymes.

(*B*) *Reduction Potentials.* Figure 5 shows the results of a potentiometric titration of AO in the presence of mediator dyes at pH 7.8. The reduction of each Fe/S center was an $n = 1$ process, with $E_m = -207$ and −310 mV for Fe/S I and Fe/S II, respectively. Table II indicates that the Fe/S I potential, when measured in the same buffer, is considerably more positive in AO than in XO or XDH (−280 mV in each). In contrast, the Fe/S II potential in AO is more negative than in XO (−245 mV) or XDH (−275 mV). Thus, whereas Fe/S II is reduced prior to Fe/S I in XO, it is reduced after Fe/S I in AO.

(*C*) *Optical Spectra.* Figure 6 shows a series of optical spectra of AO recorded after successive periods of illumination

Table II: Midpoint Reduction Potentials for Prosthetic Groups of Aldehyde Oxidase, Milk Xanthine Oxidase, and Chicken Liver Xanthine Dehydrogenase[a]

prosthetic group	potential (mV) aldehyde oxidase	xanthine oxidase	xanthine dehydrogenase
FAD/FADH·	−258	−310	−345
FADH·/$FADH_2$	−212	−220	−377
Fe/S I (ox/red)	−207	−280	−280
Fe/S II (ox/red)	−310	−245	−275
Mo^{VI}/Mo^{V} rapid[b]	−359	−355	−357
Mo^{V} rapid/Mo^{IV}	−351	−335	−337
Mo^{VI}/Mo^{V} slow[c]	−439	−354	−397
Mo^{V} slow/Mo^{IV}	−401	−386	−433

[a] Potentials were obtained by potentiometric titration of enzyme samples in 50 mM potassium phosphate, containing 1 mM EDTA, pH 7.8, at 25 °C. For details see Experimental Procedures. Data for xanthine dehydrogenase are from Barber et al. (1980). All potentials are ±15 mV and are given relative to the standard hydrogen electrode. [b] Potentials involving Mo^{V} rapid species obtained with native enzymes. [c] Potentials involving Mo^{V} slow species obtained with cyanide-treated (desulfo) enzymes.

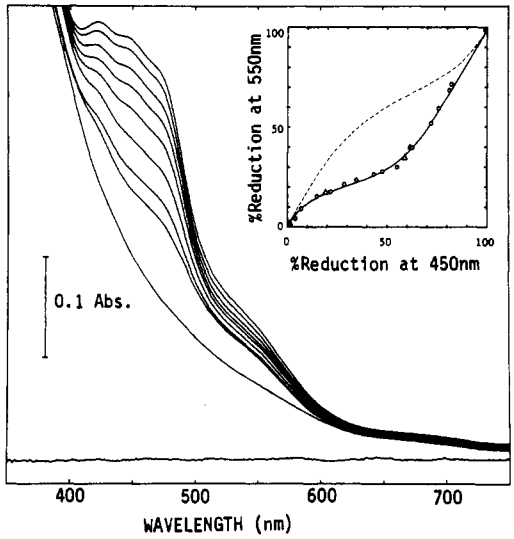

FIGURE 6: Optical spectra of photoreduced aldehyde oxidase. A solution of 6 μM AO in standard buffer containing 1 μM 5′-deazaflavin and 5 mM EDTA, in a 1-cm path-length silica cuvette, was subjected to illumination with a General Electric 200-W sealed beam lamp at 30 cm for periods of 10 s to 20 min. The solution was cooled in an ice bath during the illumination period. After each interval of illumination, optical spectra were repeatedly recorded until any slow changes had ceased. Each of the spectra shown was then recorded and the illumination repeated until eventually no further spectral changes could be detected. (Inset) ΔA_{550} plotted as a function of ΔA_{450} for various enzyme states observed during photoreduction (○) and on reduction of AO samples in EPR tubes with small amounts of $Na_2S_2O_4$ (△). The solid line represents the theoretical curve obtained by using ΔE_{450} = 12.2, 3.0, and 11.4 mM^{-1} cm^{-1}, respectively, for reduction of FAD, Fe/S I, and Fe/S II, and ΔE_{550} = 1.5 and 5.4 mM^{-1} cm^{-1}, respectively, for reduction of Fe/S I and Fe/S II in AO, together with the AO midpoint potentials of Table II. The dashed line represents the theoretical curve obtained by using the same potentials, but the ΔE_{450} and ΔE_{550} values were determined by Olson et al. (1974a) for the same centers in milk xanthine oxidase (see Table II).

of the anaerobic enzyme, in a solution containing EDTA and 5′-deazaflavin, to cause photoreduction of the enzyme prosthetic groups. Each spectrum in the figure was recorded after all slow absorbance changes (probably due to intermolecular electron transfer between enzyme molecules) had ceased. No evidence for the formation of significant amounts of flavin radical (which should be detected as increased absorbance at 610 nm) was obtained. The inset to Figure 6 shows the relationship between the absorbance changes at 450 and 550 nm as the photoreduction of AO proceeded.

Table III: Oxidized-Reduced Extinction Coefficients for the Fe/S Centers of Aldehyde Oxidase and Milk Xanthine Oxidase[a]

enzyme	oxidized-reduced Δextinction coefficients (mM^{-1} cm^{-1}) Fe/S I 450 nm	Fe/S I 550 nm	Fe/S II 450 nm	Fe/S II 550 nm
xanthine oxidase[b]	11.6	5.6	2.8	1.3
aldehyde oxidase photoreduction data	3.0	1.5	11.4	5.4
aldehyde oxidase optical/EPR data		1.8		5.4

[a] Oxidized-reduced extinction coefficients at 450 and 550 nm for the Fe/S centers in AO were obtained by fitting the photoreduction data of Figure 6 according to the procedure described by Olson et al. (1974a). Potentials of the FAD/$FADH_2$, Fe/S I (ox/red), and Fe/S II (ox/red) couples used were those given in Table II for AO. The ΔA_{450} for FAD reduction in AO was taken to be the value given by Olson et al. for xanthine oxidase, 12.2 mM^{-1} cm^{-1}. ΔE_{550} values for the Fe/S centers of AO were also obtained by measurement of optical spectra of dithionite-reduced AO samples in EPR tubes and determination of the amounts of reduced Fe/S I and Fe/S II by EPR analysis of the samples after freezing. For details see the text. [b] Olson et al. (1974a).

Olson et al. (1974b) have derived extinction coefficients for the absorbance changes on reduction of the FAD, Fe/S I, and Fe/S II centers in XO by comparing the optical changes observed in reductive titrations with the concentrations of oxidized and reduced enzyme groups determined by EPR analysis of samples frozen at various points in the titrations. Their extinction coefficients, shown in Table III, have the peculiar property that the absorbance change on reduction of Fe/S II in XO is 24% that seen on reduction of Fe/S I.

We attempted to fit the optical spectral changes seen on reduction of AO by using the Olson et al. (1974b) extinction coefficients obtained for XO with the reduction potentials obtained for the prosthetic groups of AO in the present work (Table II). The broken line in the inset to Figure 6 shows the curve expected for ΔA_{450} vs. ΔA_{550} using this method. The model clearly does not fit the data. The solid curve, which fits the data well, was obtained by using extinction coefficients nearly equal to those of Olson et al., but simply reversing the values for Fe/S I and Fe/S II in AO.

In order to check these results, we prepared partially reduced samples of AO, by addition of substoichiometric amounts of dithionite, in anaerobic EPR tubes. The optical spectrum of each sample was recorded, and the sample was then frozen, and the concentrations of reduced Fe/S I and II were determined by EPR. Table III shows the values of the extinction coefficients (ox−red) for the two Fe/S centers at 550 nm obtained by fitting the equation $\Delta A_{550} = \Delta E_{550,Fe/S\,I}[Fe/S\ I] + \Delta E_{550,Fe/S\,II}[Fe/S\ II]$ for all of the reduced samples. It can be seen that the values agree well with those expected if the extinction coefficients for XO Fe/S centers are reversed in AO. The inset to Figure 6 shows that the absorbance changes obtained from $S_2O_4^{2-}$ reduction (ΔA_{450} vs. ΔA_{550}) fall on the same curve as the data from the photoreduction experiment. We can conclude that the optical properties of the Fe/S centers in AO differ from those determined by Olson et al. (1974b) for the analogous centers in XO.

FAD. EPR signals at g = 2.0036, with the 1.9 mT line width characteristic of neutral flavin radicals (Massey & Palmer, 1966), were observed upon reduction of AO with benzaldehyde, *N*-methylnicotinamide, and dithionite and during the potentiometric titration shown in Figure 5. In the latter experiment, a maximum of 17% of the enzyme FAD was

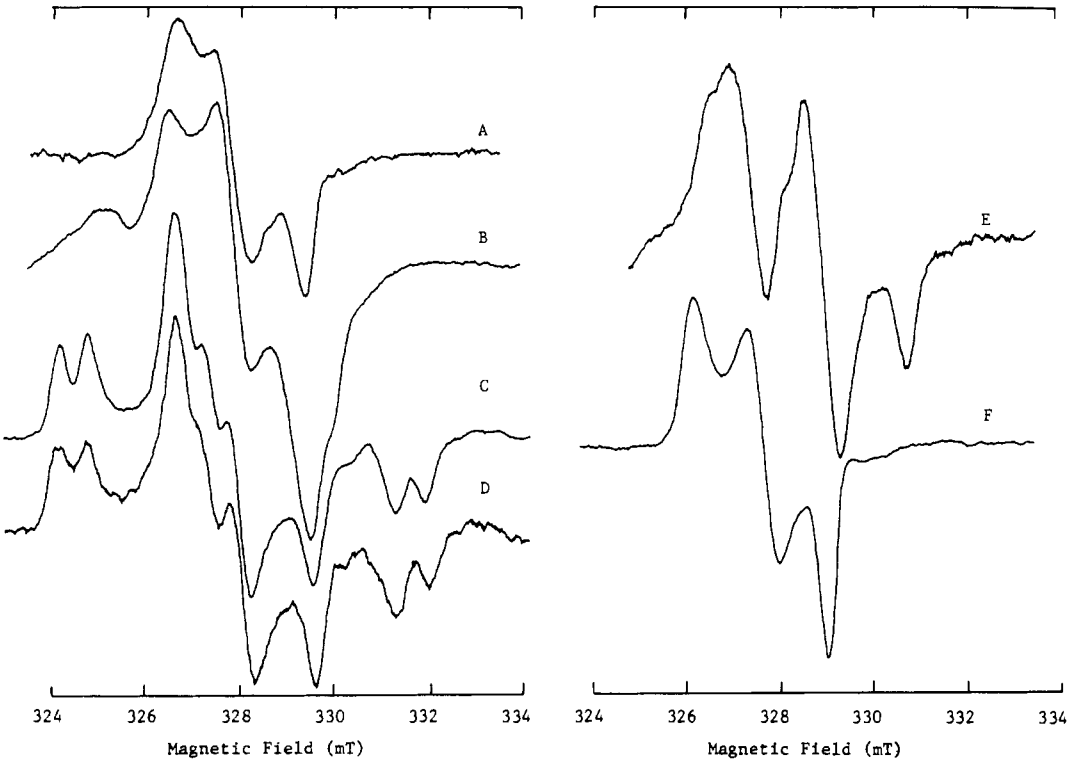

FIGURE 7: EPR spectra of Mo^V species in functional and nonfunctional forms of aldehyde oxidase. Spectra were recorded at 173 K, 9.14-GHz microwave frequency, 5-mW microwave power, and 0.25-mT modulation amplitude. (A) Resting II signal from oxidized native AO. (B) Rapid signal from native AO reduced anaerobically with 10 mM *N*-methylnicotinamide for 10 ms at 23 °C, freeze quenched, and then incubated at −50 °C for 10 min. (C) AO reacted with 150 mM formaldehyde for 20 min. (D) AO reacted with 2 mM benzaldehyde for 15 min in the presence of 750 mM methanol. (E) Cyanide-treated AO reduced with dithionite (20 mol/mol of enzyme). (F) Same as (E), but reacted for 72 h in the presence of 50% (v/v) ethylene glycol.

converted to FADH·. E_m values derived from the data of Figure 5 (Barber & Salerno, 1980) were the following: FAD/FADH·, −258 mV; FADH·/$FADH_2$, −212 mV. Table II shows that the first of these potentials is considerably more positive than that observed for FAD in either XO or XDH at the same pH, while the second potential is similar in both AO and XO, but substantially more negative in XDH. FAD is thus much more easily reduced in AO than in either of the xanthine oxidizing enzymes.

Although we have not yet been able to prepare samples of AO containing amounts of FADH· sufficient to permit microwave power saturation studies in the absence of reduced Fe/S I, the following data provide evidence for magnetic interaction between FADH· and one or both Fe/S centers in AO. $P_{1/2}$ for FADH· EPR signal (at 173 K) increased in the following manner with the percent reduction of Fe/S I and II, respectively, in AO: 48% and 0%, 0.6 mW; 72% and 0%, 0.8 mW; 86% and 20%, 1.0 mW; 100% and 52%, 1.7 mW. It should be noted that these relaxation effects are considerably smaller than those noted by Barber et al. (1982) for FADH·–reduced Fe/S interaction in XO.

Molybdenum. Figure 7 shows a number of Mo^V EPR signals observed after various treatments of AO. These signals are generally similar to those reported for XO (Bray, 1980a,b), except that no Mo^V signal is normally seen in untreated XO. The *g* and *A* values obtained for comparable signals from the two enzymes are given in Table I.

The resting II Mo^V spectrum [see Bray (1975) for terminology] is seen in untreated AO (Figure 7A). No ^1H hyperfine splitting of the spectrum could be detected. In the preparation used, this species corresponded to 5% of the enzyme Mo. Figure 5 shows that the intensity of this Mo^V signal remained unchanged when AO was poised at any potential in the range 0 to −500 mV. A Mo^V EPR species with nearly identical *g* values and similarly stable to oxidation and reduction could be generated in an amount corresponding to 50% of the AO Mo by treating desulfo AO with ethylene glycol (Figure 7F).

Treatment of AO with methanol or formaldehyde resulted in production of an "inhibited" Mo^V spectrum (Figure 7C,D) with hyperfine splittings apparently due to a single ^1H interacting with the Mo. Reduction of cyanide-treated AO resulted in formation of a Mo^V species (Figure 7E) analogous to the slow Mo^V EPR species of desulfo XO and XDH (Bray, 1980a,b).

One of the problems in working with AO has been the relatively low proportion of enzyme which contains the Mo center in a catalytically functional form (Coughlan, 1980). In the preparation used in the present work, only 30% of the AO FAD was associated with functional Mo centers. Given the factors (1) the presence of a constant background of resting II Mo^V EPR signal, (2) the fact that only a minor portion of the functional Mo can be converted to the MO^V state (see the reduction potentials in Table II), and (3) the presence of slow Mo^V EPR signal due to the desulfo Mo center (which is in fact the major form of Mo present in the AO preparation used), it has not been possible as yet to prepare pure EPR spectra of the functional Mo^V center [termed rapid by analogy with XO and XDH; see Bray (1980a,b)]. However, we have been able to obtain a rapid Mo^V EPR signal with minimal contamination by desulfo Mo^V by reacting AO for short times with substrates. The spectrum shown in Figure 7B was produced by reaction of AO with *N*-methylnicotinamide for 20 ms at 25 °C, using the freeze-quench technique, followed by incubation of the frozen sample at 223 K for 10 min. The rapid Mo^V signal, which was apparent in the 20-ms freeze-quenched sample, increased in intensity to a maximum after

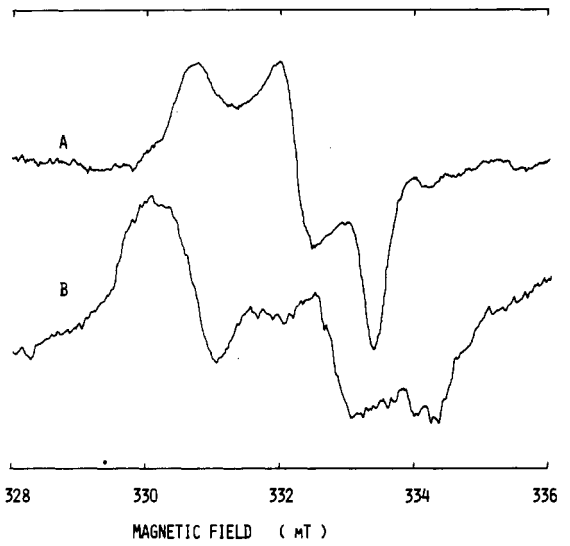

FIGURE 8: Effect of Fe/S center reduction on EPR spectrum of Mo^V in glycol-inhibited desulfo aldehyde oxidase. (A) Mo^V signal in otherwise oxidized glycol inhibited desulfo AO. (B) Mo^V signal in glycol-inhibited desulfo AO poised at −500 mV for 30 min to reduce Fe/S centers. EPR spectra were recorded at 30 K, 9.14-GHz microwave frequency, 0.5-mW microwave power, and 0.25-mT modulation amplitude.

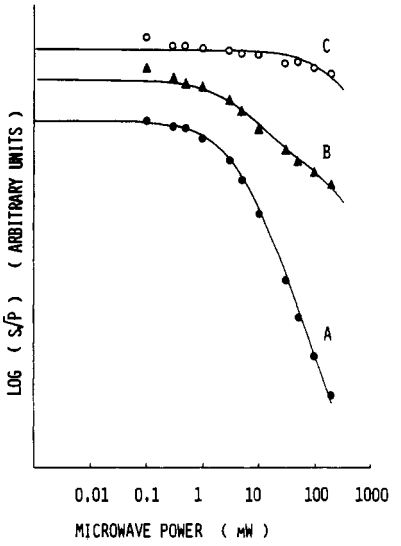

FIGURE 9: Microwave power saturation behavior of Mo^V EPR spectrum of glycol-inhibited desulfo aldehyde oxidase at various stages of Fe/S center reduction. Spectra were recorded at 103 K. (A) Oxidized enzyme. (B) Enzyme poised at −186 mV. (C) Enzyme poised at −500 mV.

further incubation at low temperature. Further incubation resulted in increasing appearance of the slow Mo^V EPR species. Because of the multiplicity of species present, we have not as yet attempted to simulate the rapid Mo^V spectrum of AO.

Figure 5 shows the behavior of the Mo^V rapid and slow EPR species on potentiometric titration of native and cyanide-treated AO. E_m for Mo^{VI}/Mo^V and Mo^V/Mo^{IV}, respectively, were the following: functional Mo, −359 and −351 mV; desulfo Mo, −439 and −401 mV. The values for functional Mo are similar to those found for XO and XDH in the same buffer (Table II). The Mo potentials in desulfo AO are more negative than those for XO; however, Barber & Siegel (1982) have found that these values show a complex pH dependence in desulfo XO, so that small changes in pK values for the various desulfo Mo reduction states in AO vs. XO could dramatically affect the observed potentials. Studies of the pH dependence of the potentials in AO have not been performed as yet.

Magnetic interaction between the Mo^V and the reduced Fe/S I center was observed in XO by two methods: (1) splitting of the Mo^V EPR spectrum at low temperature in the presence of reduced Fe/S I, but not Fe/S II (Lowe & Bray, 1978; Barber et al., 1982), and (2) a 100-fold increase in the $P_{1/2}$ for microwave power saturation of the Mo^V EPR signal at 103 K when Fe/S I (but not Fe/S II) was reduced (Barber et al., 1982). Figures 8 and 9 show the results of analogous experiments for AO. The 30 K spectrum of the normally sharp desulfo glycol inhibited Mo^V species in AO is split (Figure 8B) with respect to that of the oxidized enzyme (Figure 8A) when the enzyme is poised at a potential (−500 mV) such that both Fe/S centers are reduced. A virtually identical spectrum to that in Figure 8B was obtained with enzyme poised at −240 mV, a potential at which 80% of Fe/S, but only 10% of Fe/S II, was reduced. Figure 9 shows that the $P_{1/2}$ for saturation of this Mo^V species at 103 K, 4.5 mW in oxidized enzyme (Figure 9A), was increased to 500 mW upon reduction of both Fe/S centers (Figure 9C). Figure 9B shows the saturation behavior of Mo^V in an enzyme sample, poised at −190 mV, in which 48% of the Fe/S I was reduced, but no reduced Fe/S II could be detected. The Mo^V saturation data are readily fit by using two components, one with $P_{1/2}$ = 4.5 mV (52% of the total) and the other with $P_{1/2}$ = 500 mW (48% of the total). Thus, it is reduced center Fe/S I, and not Fe/S II, which is magnetically interacting with the Mo^V center of AO. This result indicates that the Mo–Fe/S I interaction is a common feature in AO, XO, and XDH (Lowe & Bray, 1978).

Discussion

The results of the present work show that AO contains the same types of electron-carrying groups as do XO and XDH, i.e., Mo, FAD, and two distinct types of Fe_2S_2 center. The EPR properties of the centers Fe/S I and Fe/S II are similar in all three enzymes.

The functional Mo center of AO almost certainly contains a terminal sulfur ligand since it can be reacted with cyanide to yield thiocyanate (Branzoli & Massey, 1974a) and a "desulfo" Mo species with EPR properties (in the Mo^V oxidation state) and reduction potentials similar to those described for the xanthine oxidizing enzymes (Bray, 1980a,b; Table II) which are known to contain such a Mo=S structure in the functional but not in the cyanide-treated enzyme (Bordas et al., 1980; Cramer et al., 1981). Adducts of the Mo^V center with ethylene glycol and formyl groups (derived upon reaction with formaldehyde or methanol; Bray, 1980a) yield similar EPR spectra in AO and XO.

Although the detailed EPR spectral properties of the functional Mo center are more difficult to determine, it is evident from the work of Rajagopalan et al. (1968a,b) and the present study that the Mo of AO is capable of reacting rapidly with substrates to yield rapid-type Mo^V EPR spectra analogous to those seen with XO and XDH and that the reduction potentials for the functional Mo center are similar in all three enzymes. Like the other Mo hydroxylases, AO contains the novel pterin cofactor associated with its Mo center recently described by Johnson et al. (1980).

We may conclude that, in spite of the pronounced differences in substrate specificity between AO and XO/XDH, the principal features of the Mo center are similar in the three enzymes. It is of interest that the conservation of structure near the Mo center in the three Mo hydroxylases extends to the presence of a strong Mo–Fe/S I magnetic interaction in all cases. Coffman & Buettner (1979) interpreted the strength of the interaction in XO to indicate that the Mo and Fe/S I

centers are separated by 11 ± 3 Å in that enzyme.

When we examine the detailed properties of the Fe/S and FAD centers in AO and XO/XDH, we find significant differences in these enzymes. Thus, AO Fe/S I exhibits optical spectral features more like those of XO Fe/S II than of XO Fe/S I, and the reduction potential of AO Fe/S I is considerably more positive than that of either Fe/S center in XO or XDH. While the reduction potential of Fe/S II is similar in all three enzymes in phosphate buffer at pH 7.8, the optical properties of this center in AO are like those of center Fe/S I in XO. In addition, we have been unable to detect any magnetic interaction between the Fe/S centers in AO, whereas such interaction was easily observed in XO (Barber et al., 1982). These results suggest that the detailed environments of the Fe/S centers, and possibly the steric relationships between them, are different in AO and XO.

The reduction potential of FAD is much more positive in AO at pH 7.8 than in either XO or XDH. The potentials of AO FAD, in fact, are similar to those of free flavins (Draper & Ingraham, 1968), whereas there appears to be specific stabilization of the oxidized FAD with respect to the semiquinone and hydroquinone forms in XO (i.e., E_m for FAD/FADH· is more negative in XO than in free flavin, while E_m for FADH·/$FADH_2$ is similar in XO and free flavin). Both the oxidized and semiquinone forms are stabilized with respect to the hydroquinone in the FAD center of XDH. It has been suggested that it is the low level of $FADH_2$ maintained during catalysis by XDH that accounts for its poor reactivity with O_2 relative to XO (Coughlan, 1980).

In AO, as in XO, magnetic interaction can be observed between FADH· and the Fe/S centers of the enzyme. The magnitude of the interaction, determined as relief from power saturation of the flavin radical spectrum at 173 K in the presence of reduced Fe/S, is weaker by a factor of 10 in AO compared to XO (Barber et al., 1982).

Although it is not at present possible to interpret these differences between AO and XO/XDH in detail, it is clear that the structural features of the prosthetic groups involved in transporting electrons away from the Mo center (the site of substrate oxidation/hydroxylation) may be subject to more variation in the Mo–FAD–Fe/S hydroxylases than is the structure and environment of the Mo center itself. It will be of interest to see if the Olson et al. (1974a,b) model of electron transfer in XO can be extended to the structurally similar though not identical enzyme AO.

References

Barber, M. J., & Salerno, J. C. (1980) in *Molybdenum and Molybdenum-Containing Enzymes* (Coughlan, M. P., Ed.) pp 543–568, Pergamon Press, Oxford.

Barber, M. J., & Siegel, L. M. (1982) *Biochemistry 21*, 1638–1648.

Barber, M. J., Coughlan, M. P., Kanda, M., & Rajagopalan, K. V. (1980) *Arch. Biochem. Biophys. 201*, 468–475.

Barber, M. J., Salerno, J. C., & Siegel, L. M. (1982) *Biochemistry 21*, 1648–1656.

Beinert, H., & Orme-Johnson, W. H. (1967) in *Magnetic Resonance in Biological Systems* (Ehrenberg, A., Malmstrom, B. G., & Vanngard, T., Eds.) pp 221–247, Pergamon Press, Oxford.

Bordas, J., Bray, R. C., Garner, C. G., Gutteridge, S., & Hasnain, S. S. (1980) *Biochem. J. 191*, 499–508.

Branzoli, U., & Massey, V. (1974a) *J. Biol. Chem. 249*, 4339–4345.

Branzoli, U., & Massey, V. (1974b) *J. Biol. Chem. 249*, 4346–4349.

Bray, R. C. (1975) *Enzymes, 3rd Ed. 12*, 299–419.

Bray, R. C. (1980a) *Adv. Enzymol. Relat. Areas Mol. Biol. 51*, 107–165.

Bray, R. C. (1980b) in *Biological Magnetic Resonance* (Reuben, J., & Berliner, L. J., Eds.) Vol. 2, pp 45–84, Plenum Press, New York.

Bray, R. C., & Vanngard, T. (1969) *Biochem. J. 114*, 725–735.

Cammack, R., Barber, M. J., & Bray, R. C. (1976) *Biochem. J. 157*, 469–478.

Coffman, R. E., & Buettner, G. R. (1979) *J. Phys. Chem. 83*, 2392–2400.

Coughlan, M. P. (1980) in *Molybdenum and Molybdenum-Containing Enzymes* (Coughlan, M. P., Ed.) pp 119–185, Pergamon Press, Oxford.

Cramer, S. P., Rajagopalan, K. V., & Wahl, R. (1981) *J. Am. Chem. Soc. 103*, 7721–7727.

Draper, R. D., & Ingraham, L. L. (1968) *Arch. Biochem. Biophys. 125*, 802–808.

Dutton, P. L. (1971) *Biochim. Biophys. Acta 226*, 63–80.

Felsted, R. L., Chu, A. E.-Y., & Chaykin, S. (1973) *J. Biol. Chem. 248*, 2580–2587.

Gibons, J. F., & Bray, R. C. (1968) *Biochim. Biophys. Acta 153*, 721–730.

Gutteridge, S., Tanner, S. J., & Bray, R. C. (1978) *Biochem. J. 175*, 887–897.

Johnson, J. L. (1980) in *Molybdenum and Molybdenum-Containing Enzymes* (Coughlan, M. P., Ed.) pp 345–383, Pergamon Press, Oxford.

Johnson, J. L., Hainline, B. E., & Rajagopalan, K. V. (1980) *J. Biol. Chem. 255*, 1783–1786.

Lowe, D. J. (1978) *Biochem. J. 171*, 649–651.

Lowe, D. J., & Bray, R. C. (1978) *Biochem. J. 169*, 471–479.

Lowe, D. J., Lynden-Bell, R. M., & Bray, R. C. (1972) *Biochem. J. 130*, 239–249.

Lowe, D. J., Barber, M. J., Pawlick, R. T., & Bray, R. C. (1976) *Biochem. J. 155*, 81–85.

Malthouse, J. P. G., & Bray, R. C. (1980) *Biochem. J. 191*, 265–267.

Massey, V., & Palmer, G. (1966) *Biochemistry 5*, 3181–3189.

Olson, J. S., Ballou, D. P., Palmer, G., & Massey, V. (1974a) *J. Biol. Chem. 249*, 4350–4362.

Olson, J. S., Ballou, D. P., Palmer, G., & Massey, V. (1974b) *J. Biol. Chem. 249*, 4363–4382.

Pick, F. M., McGartoll, M. A., & Bray, R. C. (1971) *Eur. J. Biochem. 18*, 65–72.

Rajagopalan, K. V., Fridovich, I., & Handler, P. (1962) *J. Biol. Chem. 237*, 922–928.

Rajagopalan, K. V., Handler, P., Palmer, G., & Beinert, H. (1968a) *J. Biol. Chem. 243*, 3784–3796.

Rajagopalan, K. V., Handler, P., Palmer, G., & Beinert, H. (1968b) *J. Biol. Chem. 243*, 3797–3806.

Tanner, S. J., Bray, R. C., & Bergmann, F. (1978) *Biochem. Soc. Trans. 6*, 1328–1330.